

# Kinetics of Catalytic Isomerization of Quadricyclane to Norbornadiene Using Near Infrared Absorption Spectroscopy: Conversion Rate and Diffusion Motion in Heterogeneous Reaction

Hsiu-Fang Fan, Thou-Long Chin, and King-Chuen Lin\*

Department of Chemistry, National Taiwan University, and Institute of Atomic and Molecular Sciences, Academia Sinica, Taipei 106, Taiwan, Republic of China

Received: February 12, 2004

By use of Fourier transform near-infrared (NIR) absorption spectroscopy and the aid of a kinetic model, we have investigated the conversion of quadricyclane to norbornadiene catalyzed by anhydrous  $\text{CuSO}_4$  and  $\text{SnCl}_2$  in chloroform. The reaction mixture is not agitated so as to avoid the effect of sample heterogeneity. The NIR absorption spectra are acquired, at a position  $\sim 2$  mm above the catalyst surface, at 30-s intervals during 4 h. The concentrations of quadricyclane and norbornadiene are determined with the analysis of partial least squares. The isomerization of quadricyclane, as numerically solved from the model, is expected to describe its behavior more accurately in the catalytic system than that obtained previously. In addition to the isomerization rate, the kinetic model takes into account the contribution of diffusion. The diffusion coefficients of quadricyclane can be determined to be  $3.8 \times 10^{-5} \text{ cm}^2 \text{ s}^{-1}$  in chloroform and  $1.14 \times 10^{-5}$  and  $2.85 \times 10^{-6} \text{ cm}^2 \text{ s}^{-1}$  inside the  $\text{CuSO}_4$  and  $\text{SnCl}_2$  stacks, respectively. Diffusion is slowed inside the solid stacks, and thus the molecular mechanism cannot be suitable for this system. Given the diffusion coefficients, the pseudo-first-order depletion rate constants are evaluated to be  $(3.7 \pm 0.1) \times 10^{-3}$  and  $(3.8 \pm 0.1) \times 10^{-3} \text{ s}^{-1}$  for  $\text{CuSO}_4$  and  $\text{SnCl}_2$ , respectively. The corresponding second-order rate constants are determined to be  $(1.3 \pm 0.2) \times 10^{-5}$  and  $(2.0 \pm 0.1) \times 10^{-6} \text{ s}^{-1} \text{ A}^{-1}$  by considering the density and the size of the catalyst particles; A denotes the total catalyst surface area per unit effective volume of solvent. The rate constant with the  $\text{CuSO}_4$  catalyst is consistent with others obtained in a continuously stirred mixture. In the surface-mediated reaction, the catalytic isomerization is subject to one-site coordination (1:1 complex) between the reactant and the catalyst. Nevertheless, a two-site coordinated reaction cannot be excluded unless the interstitial size dependence of the depletion rate is known.

## I. Introduction

The processes of photoinduced electron transfer have played a very important role in novel design of organic molecular synthesis and development of solar energy storage utilizing transition-metal complexes.<sup>1</sup> Among the applications of photoinduced electron transfer, the interconversion of quadricyclane and norbornadiene has attracted considerable attention because of its potential for solar energy storage.<sup>2,3</sup> Energy is stored when norbornadiene is photochemically converted to quadricyclane and then released when quadricyclane is catalytically converted back to norbornadiene.<sup>4–10</sup>

In a practical design of a solar energy system based on valence isomerization, the catalyst in the catalytic conversion chamber should remain insoluble in the reaction medium to avoid contamination of the other photochemical reaction chamber. To meet these requirements, transition-metal salts such as Sn, Cu, W, Mo, Co, Ni, Rh, and Pd have been considered to be potential candidates.<sup>2,7–14</sup> Among them, the cheap catalysts Sn(II) and Cu(II) salts are frequently used for investigating the kinetics of the conversion of quadricyclane to norbornadiene.<sup>7–10,15</sup> For instance, Moore and co-workers have determined the quadricyclane and norbornadiene concentrations by gas chromatography equipped with both flame ionization and mass spectroscopy detection.<sup>7</sup> Their procedure requires the removal

and analysis of aliquots of the reaction mixture at intervals during the reaction. Vickers and co-workers demonstrated with fiber-optic Raman spectroscopy the potential for automated, nondestructive, continuous monitoring of the isomerization.<sup>9</sup> Nevertheless, the suspended solids increased the sample opacity.

In recent years Fourier transform near-infrared (NIR) absorption spectroscopy has gained wide acceptance as a powerful diagnostic tool for quantitative analysis. The measurements with this technique are rapid, nondestructive, and free from contamination. With the aid of multivariate analysis, the signals, which are usually weak and severely overlap in this frequency range, can be spectrally resolved, and thus the concentrations may be accurately determined.<sup>16</sup> These properties make it suitable for application in a complex heterogeneous reaction. In our previous work, NIR absorption spectra of the isomerization reaction of quadricyclane were analyzed.<sup>10</sup> The mixtures containing the  $\text{CuSO}_4$  and  $\text{SnCl}_2$  catalysts were not stirred to avoid the effect of sample heterogeneity. The reactants diffused into the solid stacks to undergo catalytic isomerization on the metal surface. Quadricyclane and norbornadiene concentrations during the reaction were determined with the aid of the partial least squares (PLS) method. A kinetic model taking into account the diffusion was derived to give rise to the related kinetic parameters. The conversion rate constants of quadricyclane were then determined. Nevertheless, to simplify the kinetic model, a steady-state condition was assumed and the motion of quadricyclane in the solution layer was neglected.

\* To whom correspondence may be addressed. Fax: 886-2-23621483. E-mail: kclin@ccms.ntu.edu.tw.

Instead of using the approximation method, we attempt to solve numerically the kinetic model in this work. The isomerization of quadricyclane inside the catalyst layers becomes well described. In addition, we extend the previous study to the determination of diffusion coefficient of quadricyclane and then the catalytic isomerization rate constant in the heterogeneous medium. Fourier transform NIR absorption spectroscopy is used to measure the concentration of quadricyclane in the supernatant chloroform solution. Anhydrous copper(II) sulfate and tin(II) chloride are chosen as catalysts. In view of the similarity of structures and properties of the isomers, only norbornadiene is used to determine the diffusion coefficients. Then the catalytic conversion rate constant of quadricyclane is evaluated by a fit to the measured data of concentration variation. Finally, the conversion rates are compared to those reported previously.<sup>7,9,10</sup>

## II. Experimental Section

A step-scan Fourier transform spectrometer (FTS, IFS-66v/s, Bruker) equipped with a tungsten lamp as the NIR radiation source and a Si diode detector suitable for the wavelength range from 6000 to 25000  $\text{cm}^{-1}$ . The FTS contains a classical Michelson interferometer, which can be operated in either the step-scan or the rapid-scan mode with time resolution on the order of nanoseconds and milliseconds, respectively.<sup>10,17–19</sup> For the catalytic isomerization, the rapid-scan mode is fast enough for the rate determination. The interferogram of each scan, completed within milliseconds, was Fourier transformed and displayed.

The catalyst  $\text{CuSO}_4$  (Merck) or  $\text{SnCl}_2$  (Janssen) weighing 4–19 g was added in a cuboid cell (1 cm  $\times$  5 cm  $\times$  4.8 cm), placed in the compartment of the FTS, followed by slow addition of the chloroform solvent up to an appropriate height, and was left to stand for 1 h to reach equilibrium. The light beam was passed through an iris of 2-mm diameter prior to propagation through the solvent layer  $\sim$ 2 mm above the solid surface. The NIR spectrum of solvent background was acquired. Then aliquots of chloroform from the solvent layer were well mixed with 30–50  $\mu\text{L}$  quadricyclane or norbornadiene and carefully returned to the sample cell. Since the suspended salts had settled in the cell, the effect of light scattering and sample opacity was minimized. NIR spectra were recorded at 30-s intervals over a period of 4 h. Each spectrum was an average of 10 measurements.

The reactant quadricyclane (quadricyclo[2.2.1.0.0] heptane) was photosynthesized from norbornadiene (bicyclo[2.2.1] hepta-2,5-diene). Its purity was examined by  $^1\text{H}$  NMR spectroscopy. Norbornadiene (99%, Aldrich) was used without further purification. The catalysts  $\text{SnCl}_2$  and  $\text{CuSO}_4$  were heated at 140  $^\circ\text{C}$  for 12 h before use.  $\text{CHCl}_3$  was dried over molecular sieves with 4- $\text{\AA}$  pore size. The concentrations of quadricyclane and norbornadiene were in the range of 0.005–0.100 M (mol/L) for the partial least-squares analysis.

## III. Kinetic Model

Following diffusion into the solid stacks, the quadricyclane molecules are adsorbed on the catalyst surface, by either one-site and/or two-site coordination, to result in norbornadiene. The kinetic rate equation including the rate of diffusion can be expressed as<sup>20</sup>

$$\frac{dC}{dt} = D \frac{d^2C}{dx^2} - kC \quad (1)$$

where  $C$  is the concentration of quadricyclane,  $D$  its diffusion

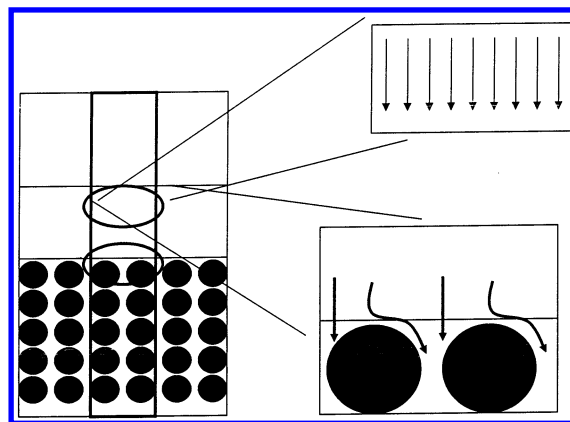


**Figure 1.** Schematic of the diffusion motion of quadricyclane in the solution layer and inside the stacks of catalyst. One-dimensional diffusion motion is assumed in the solution, but the motion is slowed by obstacle of solid stacks.

coefficient, and  $x$  the depth measured from the top of the solution to the bottom of the cell.

In our earlier work, the steady-state approximation was applied to eq 1, i.e.,  $dC/dt = 0$ .<sup>10</sup> Accordingly, the time-dependent concentration of quadricyclane can be expressed by two terms, one containing the reaction rate and the other the diffusion contribution. The fit to the experimental results yields a pseudo-first-order rate constant and a diffusion-related parameter. In this work, eq 1 was solved numerically using a program based on Matlab 6.5 for which the following input data are required. First, the boundary conditions,  $dC/dx = 0$ , are set at the top level of solution ( $x$  is defined as zero) and the bottom of the cell. Then, the data for the height of solvent above the catalyst surface and the effective depth of the catalyst stacks should be given. Note that the effective depth of the catalyst reflects the solvent amount in the interstices of the solid stacks. It can be evaluated by measuring the additional height of the solvent layer when a given weight of catalyst is deposited in the cell.

For simulation with eq 1, two stages are followed. Initially, isomerization of quadricyclane depends on the diffusion alone. Once the solution has moved into the solid stacks, the rate of quadricyclane disappearance is affected by both diffusion and chemical reaction. At this stage, eq 1 is solved involving both factors. For one-dimensional diffusion, the rate is different in the solution layer and the catalyst stacks. The diffusion of quadricyclane may be hindered while moving through the catalyst stacks. Figure 1 shows a schematic to describe the different behavior in the two phases. When the catalyst is packed more tightly, the diffusion in the downward direction becomes slower.<sup>21</sup>

According to the above simulation processes, given the boundary conditions and the required data, an example of the time- and position-dependent concentration distribution of the reactant is shown in Figure 2. Each curve indicates the concentration distribution in the solution layer and inside the catalyst stacks. The position of the interface between these two phases is set at  $x = 0.8$  cm. To find the role of the reaction rate, the concentration distributions are evaluated with and without involvement of the reaction term. Figure 2a shows that the isomerization of quadricyclane is dominated by the diffusion alone for the entire system. The concentration change appears to be slower, as compared to the case when a reaction rate is included (Figure 2b). To compare with the experimental observation of the reactant decay, each time-dependent simulated curve is integrated within the zone where the NIR probe beam

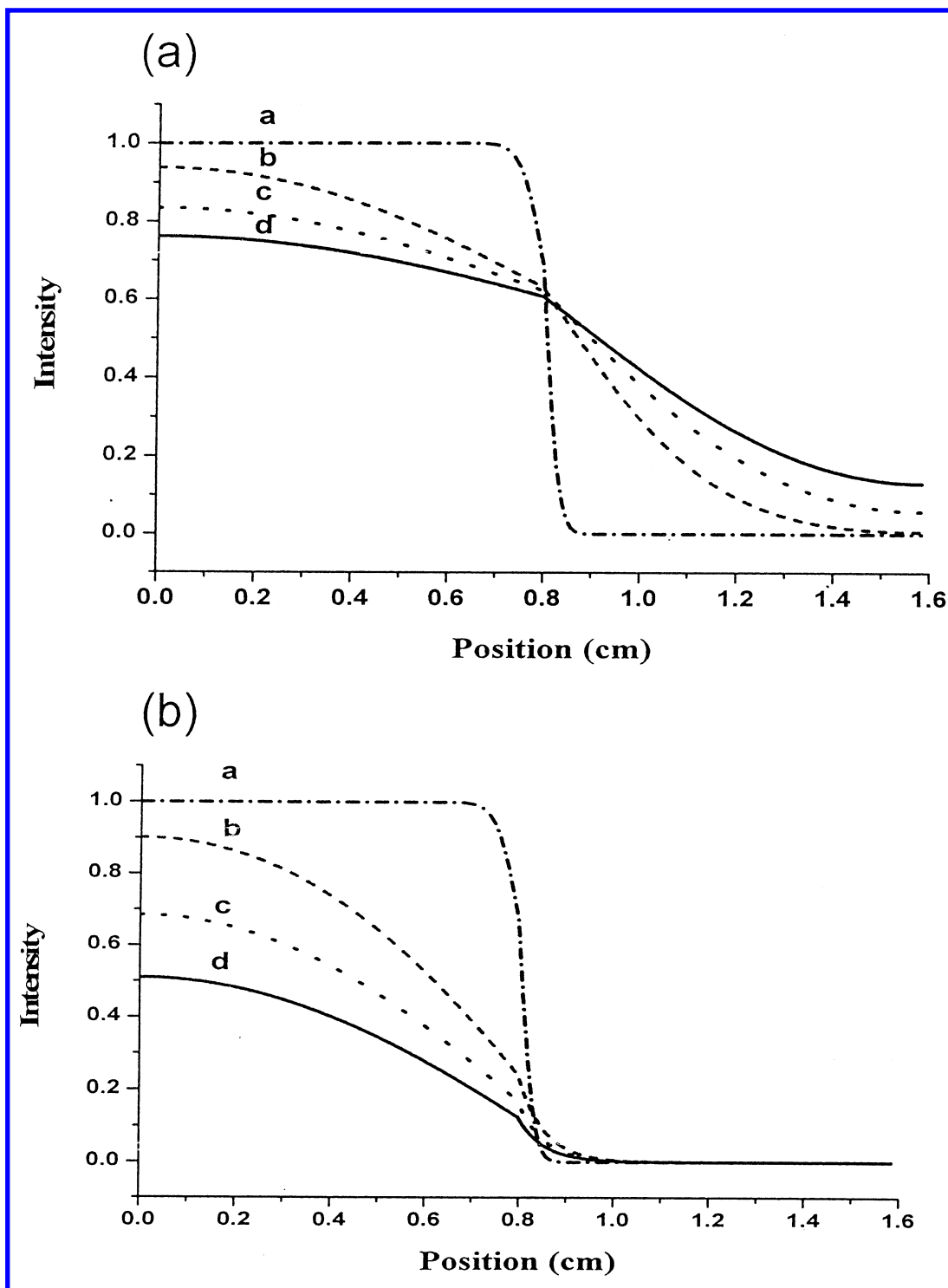


**Figure 2.** (a) Simulated curves for time-dependent concentration of quadricyclane at times of (a) 30 s, (b) 1 h, (c) 2 h, and (d) 3 h, respectively, with the diffusion coefficients assumed to be  $3.8 \times 10^{-5}$  and  $1.14 \times 10^{-6} \text{ cm}^2 \text{ s}^{-1}$  in the solution layer and the catalyst stacks, respectively. (b) Simulated curves for time-dependent concentration of quadricyclane under the same conditions except that of the reaction rate constant of  $3.6 \times 10^{-3} \text{ s}^{-1}$  are included. The position for the top level of solution layer is defined as  $x = 0 \text{ cm}$ , and the interface between the liquid and solid phases is positioned at  $x = 0.8 \text{ cm}$ .

propagates through the solution. Given the experimental conditions, the parameters of the diffusion coefficient and the depletion rate constant of quadricyclane can be optimized simultaneously to fit the obtained decay curve.

#### IV. Results and Discussion

**A. Determination of Isomer Concentrations.** Parts a and b of Figure 3 show the NIR spectra for isomerization of quadri-

cyclane to norbornadiene catalyzed by  $\text{CuSO}_4$  and  $\text{SnCl}_2$ , respectively, at reaction times of 10, 60, 120, 180, and 240 min. The NIR spectra of quadricyclane and norbornadiene in chloroform peak at 8840 and 8900  $\text{cm}^{-1}$ , respectively, while the NIR spectra of the solvent spread from 8000 to 11 500  $\text{cm}^{-1}$ . When the solvent background spectrum is subtracted, only the band at 8700  $\text{cm}^{-1}$  leaves minor noise in the baseline. In comparison, when benzene was the solvent, as in the previous

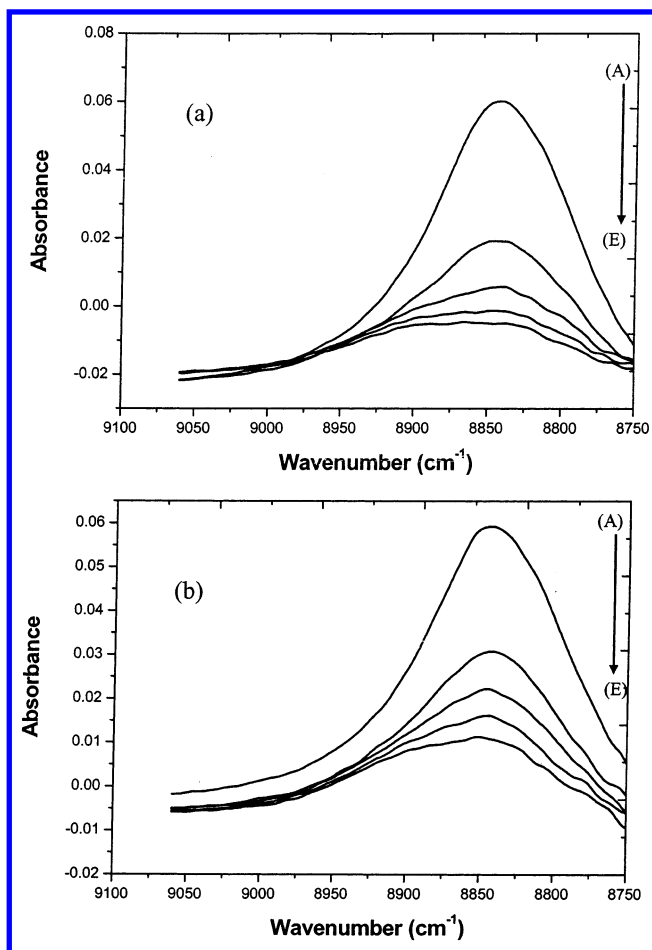


**Figure 3.** (a) The NIR spectra for isomerization of quadricyclane to norbornadiene in chloroform, with the solvent background subtracted, catalyzed by  $\text{CuSO}_4$  over a reaction period of (a) 10, (b) 60, (c) 120, (d) 180, and (e) 240 min, respectively. (b) The NIR spectra for isomerization of quadricyclane to norbornadiene in chloroform, with the solvent background subtracted, catalyzed by  $\text{SnCl}_2$  at (a) 10, (b) 60, (c) 120, (d) 180, and (e) 240 min, respectively.

work, the quadricyclane and norbornadiene absorptions were obscured by the large noise level in the  $8540\text{--}8850\text{-cm}^{-1}$  region, even after background subtraction.<sup>10</sup>

With the aid of the partial least-squares method, the small difference shown in the absorption bands (Figure 3) allows determination of the individual concentrations of quadricyclane and norbornadiene.<sup>22–24</sup> In this work, 480 sets of the NIR absorption spectra for each catalytic reaction system were acquired, while 56 calibration sets of various concentration combinations of quadricyclane and norbornadiene each in the range of  $0.005\text{--}0.100\text{ M}$  were made. Either quadricyclane or norbornadiene concentration in the reaction mixture could be determined by a fit of the calibration sets to the observed spectra.<sup>22–24</sup> As shown in Figure 4, the fit between the predicted and actual concentrations is characterized by a straight line with slope = 1.00 and a regression coefficient  $> 0.98$ , thereby ensuring reliability of the determined concentrations.

**B. Determination of Diffusion Coefficient and Reaction Rate Constants.** According to the kinetic model, the diffusion coefficients and the reaction rate constant can be approximately determined simultaneously by a best fit to the experimental time-dependent concentration of quadricyclane. When these parameters are evaluated separately, the quality of simulation is improved. Nevertheless, the quadricyclane concentrations cannot be used for determining the diffusion coefficients when the

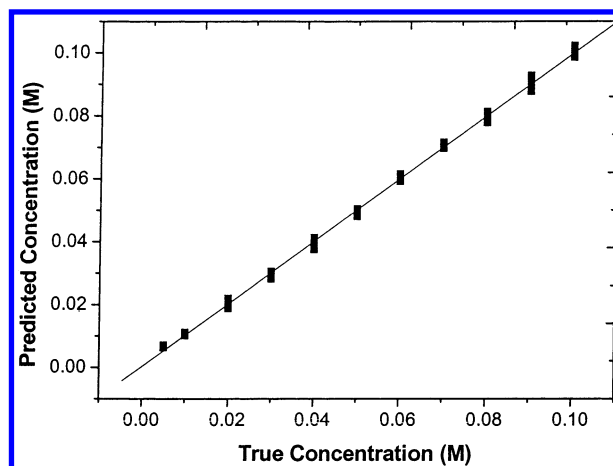


**Figure 4.** Calibration plot for determination of quadricyclane concentration from the mixtures of quadricyclane and norbornadiene in the range of  $0.005\text{--}0.100\text{ M}$  in chloroform.

catalysts are present. Since the product norbornadiene has a similar structure and properties to quadricyclane, it may be used as a substitute to determine the diffusion coefficients for quadricyclane in the catalytic system.

Similarly, 20 calibration sets of the norbornadiene solutions in the range of  $0.005\text{--}0.100\text{ M}$  were used in determining the diffusion coefficients. Comparison of the calibration sets with the observed time-dependent spectra of norbornadiene solutions caused by diffusion using the PLS analysis yields the corresponding concentration of norbornadiene. The measured concentration change due to diffusion is plotted in Figure 5. To simulate the diffusion, eq 1 containing only the diffusion term is solved as described in Kinetic Model section. The following measured data are also required for the simulation: the height of solution layer and the effective depth of catalyst stacks. As shown in Figure 5, the diffusion coefficients of quadricyclane in solution and inside the catalyst stacks are thus evaluated by a fit to the observed concentration change of norbornadiene. To confirm reliability of the obtained parameters, the solution volume is changed, i.e., the height of the solution layer is set at different values; the results remain consistent. As listed in Table 1, the diffusion coefficients in solvent and in the presence of  $\text{CuSO}_4$  and  $\text{SnCl}_2$  catalysts are thus determined to be  $3.8 \times 10^{-5}$ ,  $1.14 \times 10^{-5}$ , and  $2.85 \times 10^{-6}\text{ cm}^2\text{ s}^{-1}$ , respectively. To the best of our knowledge, the diffusion coefficients for either quadricyclane or norbornadiene in chloroform have not been reported previously. Diffusion coefficients for the structural analogues, toluene or benzene (each radius assumed to be  $1.5\text{ \AA}$ ) in chloroform, evaluated to be  $2.7 \times 10^{-5}\text{ cm}^2\text{ s}^{-1}$  at  $25^\circ\text{C}$ ,<sup>25</sup> are of the same order of magnitude as those in our work.

Let us see what may happen if the diffusion coefficients are assumed to be identical in the two phases. The case of the  $\text{CuSO}_4$  system is used as an example. Figure 5a shows that the quality of the fit to the observation becomes poor, yielding a value of  $1.15 \times 10^{-5}\text{ cm}^2\text{ s}^{-1}$ . When  $\text{SnCl}_2$  is substituted, the fit yields a value of  $3.47 \times 10^{-6}\text{ cm}^2\text{ s}^{-1}$ . The determined values are different when the experimental conditions change.

Diffusion inside the solid stacks depends on the size of the interstices between the catalyst particles. If the spaces are larger than the mean free path, the distance that a molecule moves between collisions, then the molecular motion is the same as in the solvent, neglecting disturbance by the catalyst. Such behavior is characterized by the molecular mechanism.<sup>21</sup> When the size decreases and the catalyst stack becomes more tightly packed, diffusion tends to be slower. The effect of size can be described



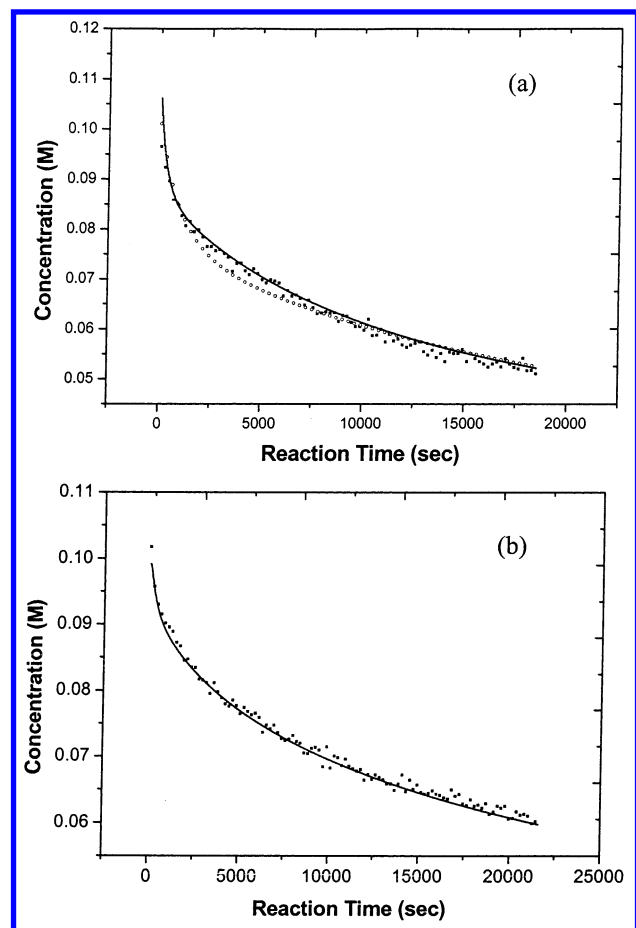


**Figure 5.** (a) Time-dependent concentration of norbornadiene caused by diffusion in chloroform in the presence of  $\text{CuSO}_4$ . The measurements with the (■) are conducted at the solution height of 0.55 cm and the catalyst weight of 8 g. The solid line indicates the corresponding fit to yield the appropriate diffusion coefficients in the solution layer and the solid stacks. The fit with the (○) yields a value of  $1.15 \times 10^{-5} \text{ cm}^2 \text{ s}^{-1}$  for the diffusion coefficients identical in the solution layer and the catalyst stacks. (b) Time-dependent concentration of norbornadiene caused by diffusion in chloroform in the presence of  $\text{SnCl}_2$ . The measurements with the (■) symbol are conducted at the solution height of 0.5 cm and the catalyst weight of 19 g. The solid line indicates the corresponding fit to yield the appropriate diffusion coefficients in solution layer and solid stacks.

**TABLE 1: Diffusion Motion of Norbornadiene in Chloroform with  $\text{CuSO}_4$  and  $\text{SnCl}_2$  as Catalysts**

catalyst	catalyst weight (g)	solution height (cm)	$D_1 \times 10^5$ <sup>a</sup> ( $\text{cm}^2 \text{ s}^{-1}$ )	$D_2 \times 10^5$ <sup>b</sup> ( $\text{cm}^2 \text{ s}^{-1}$ )
$\text{CuSO}_4$	8	0.55	3.8	1.14
	8	0.65	3.8	1.14
$\text{SnCl}_2$	19	0.5	3.8	0.285
	19	0.45	3.8	0.285

<sup>a</sup>  $D_1$  denotes the diffusion coefficient in chloroform. <sup>b</sup>  $D_2$  denotes the diffusion coefficient in catalyst.

by a geometry factor, defined as the ratio of the diffusion coefficient in the catalyst to that in the solvent. It is found to be 0.3 and 0.075 for  $\text{CuSO}_4$  and  $\text{SnCl}_2$ , respectively. The latter catalyst is packed more tightly so that diffusion is relatively more difficult.

Given the diffusion coefficients in the two phases, the isomerization rate constant of quadricyclane can be evaluated by simulating the concentration decrease in the catalytic reaction. The obtained time-dependent spectra of isomerization catalyzed by either  $\text{CuSO}_4$  or  $\text{SnCl}_2$  may yield the corresponding

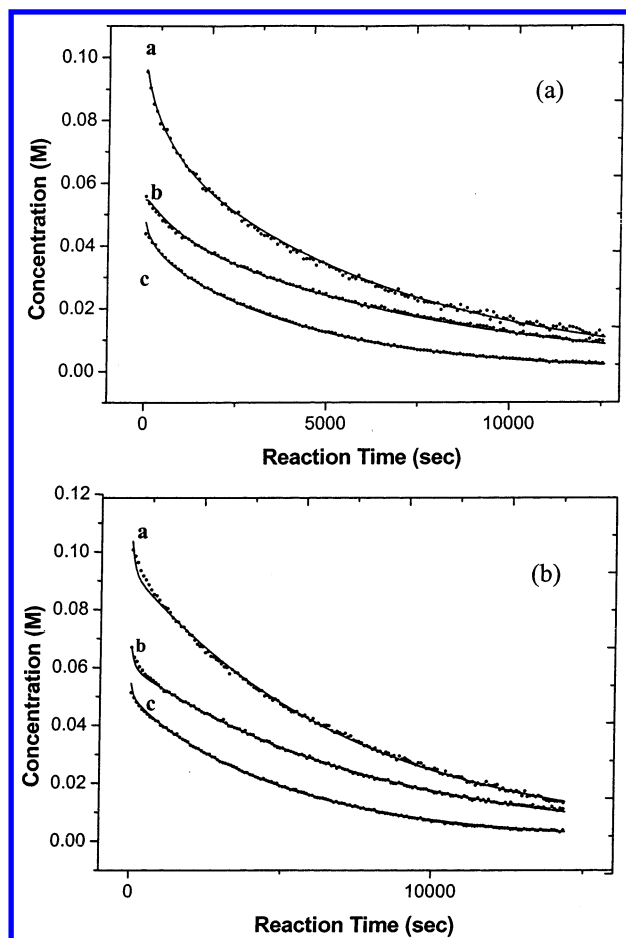


**Figure 6.** (a) Reaction time dependence of concentration of quadricyclane catalyzed by 4.5 g  $\text{CuSO}_4$  in chloroform with solution heights of (a) 0.45, (b) 0.7, and (c) 0.65 cm. The solid lines indicate the corresponding simulated curves with the diffusion coefficients fixed at  $3.8 \times 10^{-5}$  and  $1.14 \times 10^{-5} \text{ cm}^2 \text{ s}^{-1}$  in the solution layer and the solid stacks, respectively. The fit yields the depletion rate constant of quadricyclane. (b) Reaction time dependence of concentration of quadricyclane catalyzed by 14 g  $\text{SnCl}_2$  in chloroform with solution heights of (a) 0.5, (b) 0.55, and (c) 0.4 cm. The solid lines indicate the corresponding simulated curves with the diffusion coefficients fixed at  $3.8 \times 10^{-5}$  and  $2.85 \times 10^{-6} \text{ cm}^2 \text{ s}^{-1}$  in the solution layer and the solid stacks, respectively. The fit yields the depletion rate constant of quadricyclane.

concentrations of quadricyclane by the partial least-squares fit. Figures 6 and 7 show the results of the concentration change of the reactant over a reaction time of 3 h. By adjusting the reaction rate constant, the simulated time consumption of quadricyclane can be fit to the experimental data. To inspect the reliability of the kinetic model and the accuracy of the obtained rate constants, the amounts of solvent and catalysts are varied in the simulation. As listed in Tables 2 and 3, the results are consistent under varied experimental conditions. Figures 6 and 7 show the best fit for different amounts of solvent and catalysts, respectively. The obtained pseudo-first-order reaction rate constants are  $(3.6 \pm 0.1) \times 10^{-3} \text{ s}^{-1}$  for  $\text{CuSO}_4$  and  $(3.7 \pm 0.1) \times 10^{-3} \text{ s}^{-1}$  for  $\text{SnCl}_2$ .

**C. Comparison with Other Experiments.** In a similar heterogeneous catalytic reaction, Moore and co-workers suggested that both one-site and two-site coordination of quadricyclane may lead to the production of norbornadiene. The depletion rate of quadricyclane can be expressed as<sup>7</sup>

$$\frac{dQ}{dt} = [k_1^{\text{II}}W + k_2^{\text{II}}W^2]Q \quad (2)$$

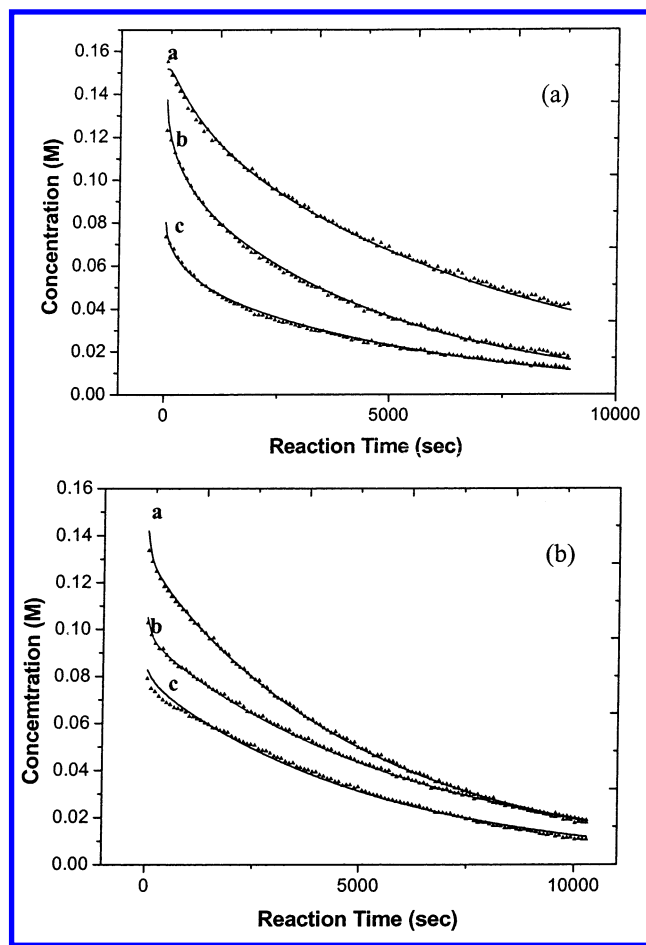


**Figure 7.** Reaction time dependence of concentration of quadricyclane isomerization in the presence of  $\text{CuSO}_4$  in chloroform with catalyst amounts and solution heights of (a) 4.5 g and 0.65 cm, (b) 6 g and 0.5 cm, and (c) 8 g and 0.55 cm, respectively. The solid lines are simulated with diffusion coefficients fixed at  $3.8 \times 10^{-5}$  and  $1.14 \times 10^{-5} \text{ cm}^2 \text{ s}^{-1}$  in the solution layer and the solid stacks, respectively. The fit yields the depletion rate constant of quadricyclane. (b) Reaction time dependence of concentration of quadricyclane catalyzed by  $\text{SnCl}_2$  in chloroform with catalyst amounts and solution heights of (a) 14 g and 0.4 cm, (b) 17 g and 0.45 cm, and (c) 19 g and 0.4 cm, respectively. The solid lines indicate the corresponding simulated curves with the diffusion coefficients fixed at  $3.8 \times 10^{-5}$  and  $2.85 \times 10^{-6} \text{ cm}^2 \text{ s}^{-1}$  in the solution layer and the solid stacks, respectively. The fit yields the depletion rate constant of quadricyclane.

**TABLE 2: Kinetic Data of Quadricyclane Catalyzed by  $\text{CuSO}_4$**

catalyst weight (g)	solution height (cm)	$D_1 \times 10^5$ <sup>a</sup> ( $\text{cm}^2 \text{ s}^{-1}$ )	$D_2 \times 10^5$ <sup>b</sup> ( $\text{cm}^2 \text{ s}^{-1}$ )	$k_1 \times 10^3$ <sup>c</sup> ( $\text{s}^{-1}$ )	$k_{II} \times 10^5$ <sup>d</sup> ( $\text{s}^{-1} \text{ A}^{-1}$ )
4.5	0.45	3.8	1.14	3.6	1.3
4.5	0.7	3.8	1.14	3.8	1.4
4.5	0.65	3.8	1.14	3.7	1.3
6	0.5	3.8	1.14	3.5	1.3
8	0.55	3.8	1.14	3.7	1.4

<sup>a</sup>  $D_1$  denotes the diffusion coefficient in chloroform. <sup>b</sup>  $D_2$  denotes the diffusion coefficient in catalyst. <sup>c</sup>  $k_1$  denotes the pseudo-first-order catalytic rate constant. <sup>d</sup>  $k_{II}$  denotes the second-order catalytic rate constant; A denotes the total catalyst surface per unit effective volume of solvent as defined in text.

where  $Q$  denotes the quadricyclane concentration and  $W$  the weight of catalyst. They have determined the one-site and two-site coordinated rate constants,  $k_1^{\text{II}}$  and  $k_2^{\text{II}}$ , to be  $2.9 \times 10^{-2} \text{ min}^{-1} \text{ g}^{-1}$  and  $7.3 \times 10^{-2} \text{ min}^{-1} \text{ g}^{-2}$ , respectively, for the  $\text{CuSO}_4$  catalyst in benzene by the detection with gas chromatography mass spectrometry.<sup>7</sup> They also found that with smaller

**TABLE 3: Kinetic Data of Quadricyclane Catalyzed by  $\text{SnCl}_2$**

catalyst weight (g)	solution height (cm)	$D_1 \times 10^5$ <sup>a</sup> ( $\text{cm}^2 \text{ s}^{-1}$ )	$D_2 \times 10^6$ <sup>b</sup> ( $\text{cm}^2 \text{ s}^{-1}$ )	$k_1 \times 10^3$ <sup>c</sup> ( $\text{s}^{-1}$ )	$k_{II} \times 10^6$ <sup>d</sup> ( $\text{s}^{-1} \text{ A}^{-1}$ )
14	0.5	3.8	2.85	3.5	1.9
14	0.55	3.8	2.85	3.7	2.0
14	0.4	3.8	2.85	4.1	2.2
17	0.45	3.8	2.85	3.6	2.0
19	0.4	3.8	2.85	3.8	2.1

<sup>a</sup>  $D_1$  denotes the diffusion coefficient in chloroform. <sup>b</sup>  $D_2$  denotes the diffusion coefficient in catalyst. <sup>c</sup>  $k_1$  denotes the pseudo-first-order catalytic rate constant. <sup>d</sup>  $k_{II}$  denotes the second-order catalytic rate constant; A denotes the total catalyst surface per unit effective volume of solvent as defined in text.

amounts of  $\text{CuSO}_4$  the isomerization is dominated by a one-site coordination, but as the amount of catalyst increases, the two-site coordination becomes dominant.

For comparison, the total rate constant,  $k_{\text{tot}}$ , in eq 2 is modified as

$$\begin{aligned}
 k_{\text{tot}} &= k_1^{\text{II}} W + k_2^{\text{II}} W^2 \\
 &= k_1 \frac{\Delta A}{\Delta V_e} + k_2 \left( \frac{\Delta A}{\Delta V_e} \right)^2 \\
 &= k_1 \frac{6W}{da\Delta V_e} + k_2 \left( \frac{6W}{da\Delta V_e} \right)^2 \quad (3)
 \end{aligned}$$

where  $\Delta A$  is the total surface area of the solid,  $\Delta V_e$  the effective volume of solvent squeezed in the catalyst stacks,  $d$  the density of catalyst, and  $a$  the average diameter of the particles. The effective volume of solvent inside the catalyst stacks is readily evaluated from the bottom-side area of the cell multiplied by the additional height of the solvent layer when the catalyst is added. Given the evaluated effective solvent volume 2.7 mL (i.e.,  $1 \times 5 \times 0.54 \text{ cm}^3$ ), the weight 4.5 g of catalyst, the density  $3.6 \text{ g/cm}^3$  of anhydrous  $\text{CuSO}_4$  with the average diameter  $1.0 \times 10^{-2} \text{ cm}$  (140–200 mesh selected), and the pseudo-first-order rate constant  $3.6 \times 10^{-3} \text{ s}^{-1}$  obtained from our experiments with the  $\text{CuSO}_4$  catalyst, the second-order rate constant,  $k_1$ , is estimated to be  $1.3 \times 10^{-5} \text{ s}^{-1} \text{ A}^{-1}$ . A denotes the total catalyst surface area per unit effective volume of solvent. If a one-site coordinated reaction is assumed and the effective volume of solvent is replaced by the total volume, 10 mL, used in a stirred solution,<sup>7</sup> then our value would be  $1.3 \times 10^{-6} \text{ s}^{-1} \text{ cm}^{-2}$  or  $4.4 \times 10^{-4} \text{ s}^{-1} \text{ g}^{-1}$ , consistent with  $1.1 \times 10^{-6} \text{ s}^{-1} \text{ cm}^{-2}$  or  $4.8 \times 10^{-4} \text{ s}^{-1} \text{ g}^{-1}$  given by Moore and co-workers.<sup>7</sup> Nevertheless, if the contribution of two-site coordination is included, the obtained second-order rate constant  $k_1$ , based on exclusive one-site coordination, may become smaller.

In another similar experiment, Vickers and co-workers used Raman spectroscopy to study the kinetic behavior of quadricyclane and norbornadiene.<sup>9</sup> They determined the limit of detection of the norbornadiene product but did not derive the depletion rate constant of quadricyclane. From the profile of the time-dependent concentration of quadricyclane that they demonstrated, the initial rate, as divided by the initial concentration of 0.0997 M and the weight 0.375 g of  $\text{CuSO}_4$  catalyst, may lead to a second-order depletion rate constant of  $2.7 \times 10^{-2} \text{ min}^{-1} \text{ g}^{-1}$ , consistent with  $k_1^{\text{II}} = 2.9 \times 10^{-2} \text{ min}^{-1} \text{ g}^{-1}$  given by Moore and co-workers<sup>7</sup> and the results in this work.

As compared to our early work,<sup>10</sup> several different aspects may be noted. First, in the previous work, a steady-state approximation was assumed and the boundary conditions,  $dC/dx = 0$ , were applied to the top and the bottom levels of the

catalyst stacks. Accordingly, the kinetic equation was simplified into two separate terms containing chemical reaction and diffusion contribution. This model neglects the role played by the solution layer, where the absorption of quadricyclane is measured. Second, the molecular mechanism for the diffusion motion was assumed previously, but only a diffusion-related parameter in the catalyst stacks was determined. In contrast, explicit values of diffusion coefficients in solution and inside the catalyst stacks are determined in this work. The packing of catalyst turns out to decrease the diffusion flow. The quadricyclane diffusion inside the catalyst layer cannot simply be assumed to be the same as in the solution layer. Third, the pseudo-first-order rate constant previously obtained depended on the weight of catalyst.<sup>10</sup> However, the pseudo-first-order rate constant obtained in this work is independent of the catalyst amount. The reason lies in the different design of reactors. With previous use of a cylindrical cell aligned horizontally, the top solid surface area may increase with the gradual deposition of the catalyst. Therefore, the increased catalyst amount, previously used in the range of 0.2–1.2 g,<sup>10</sup> may lead to an increase of the surface area contacted with quadricyclane. The pseudo-first-order rate constant appears to increase with the catalyst amount. In contrast, in the cuboid cell used in this work, the top surface area remains constant no matter how much the catalyst increases. The effective solvent volume in the catalyst particle interstices is proportional to the amount of catalyst. Thus, the total surface area of catalyst per unit volume of solvent remains constant. Unless the particle size changes with consequent change in the packing, the pseudo-first-order rate constant does not depend on the weight of catalyst provided the same cuboid cell is used. To confirm this point, a preliminary result for the size dependence of the pseudo-first-order rate constant is recently obtained, yielding a straight line with the slope indicative of the second-order rate constant.<sup>26</sup>

The resultant second-order depletion rate constant with the CuSO<sub>4</sub> catalyst in this work is an order of magnitude larger than the value of  $2.3 \times 10^{-5} \text{ s}^{-1} \text{ g}^{-1}$  reported in our early work.<sup>10</sup> The depletion rate constant of quadricyclane is believed to be more accurate herein, since the simulation method considering the influence of the solution layer should more truly reflect the experimental procedures and consequences. Another possible reason for the lower value obtained previously is related to the catalyst amount. The one-site coordinated reaction may be simplified as



During the surface-mediated reaction, the quadricyclane, Q, is first adsorbed on the catalyst surface to form the QS complex, and then the converted norbornadiene, N, is released from the solid surface. For a concentration 0.1 M (10 mL) of quadricyclane and the weight 1 g of CuSO<sub>4</sub> catalyst used in the previous work,<sup>10</sup> each converted particle numbers correspond to  $6 \times 10^{20}$  and  $4 \times 10^{21}$ , respectively. When considering the cluster size of the catalyst, the effective number for one-site coordination may be reduced considerably. Thus, the depletion rate of the reactant (in the  $k_1$  process) may be decreased by limited effective sites on the catalyst surface, depending on the desorption rate of the product (in the  $k_2$  process). When the amount of catalyst is sufficiently large as in this work, the effective sites on the catalyst surface exceed the reactant molecules. The quadricyclane may be adsorbed freely on the catalyst surface, thereby leading to enhancement of the depletion rate.

## V. Conclusion

By use of Fourier transform NIR absorption spectroscopy combined with a new simulation model, we have studied the kinetic behavior for isomerization of quadricyclane catalyzed by anhydrous CuSO<sub>4</sub> and SnCl<sub>2</sub>. For this heterogeneous reaction, the reaction mixture is not agitated and the NIR radiation is positioned to pass through the solution above the solid surface. The kinetic model contains contributions of diffusion and isomerization. The depletion of quadricyclane, as numerically solved from the model, may describe the behavior of quadricyclane in the catalytic system more accurately than the method used previously. Diffusion coefficients of quadricyclane in the solution and inside the catalyst stacks can be explicitly determined. The results suggest that the diffusion is slower within the catalyst, and thus the molecular mechanism is not applicable in this system. The pseudo-first-order depletion rate constant is independent of the weight of catalyst. Our reaction rates are consistent with others obtained in a continuously stirred mixture. In this surface-mediated reaction, the isomerization of quadricyclane is primarily controlled via one-site coordination between the reactant and the catalyst, but a contribution of a two-site coordinated reaction cannot be excluded. The spectroscopic technique and simulation method developed in this work should be a useful addition to the kinetic studies of heterogeneous catalysis.

**Acknowledgment.** This work is supported by the National Science Council of the Republic of China under Contract No. NSC 91-2113-M-002-033. The authors wish to thank Prof. T. I. Ho for providing the synthesized quadricyclane.

## References and Notes

- (1) Mattay, J. *Topics in Current Chemistry: Photoinduced Electron-Transfer I*; Springer-Verlag: Berlin, 1990; pp 21–58.
- (2) Hautala, R. R.; King, R. B.; Kutal, C. *Solar Energy: Chemical Conversion and Storage*; Humana Press: Clifton, NJ, 1979; pp 333–344.
- (3) Bren, V. A.; Dubonosov, A. D.; Minkin, V. I.; Chernov, V. A. *Russ. Chem. Rev.* **1991**, 60, 451.
- (4) Cuppoletti, A.; Dinnocenzo, J. P.; Goodman, J. L.; Gould, I. R. *J. Phys. Chem. A* **1999**, 103, 11253.
- (5) Sluggett, G. W.; Turro, N. J.; Roth, H. D. *J. Phys. Chem. A* **1997**, 101, 8834.
- (6) Franceschi, F.; Guardigli, M.; Solari, E.; Floriani, C.; Chiesi, V. A.; Rizzoli, C. *Inorg. Chem.* **1997**, 36, 4099.
- (7) Fife, D. J.; Morse, K. W.; Moore, W. M. *J. Am. Chem. Soc.* **1983**, 105, 7404.
- (8) Patrick, T. B.; Bechtold, D. S. *J. Org. Chem.* **1984**, 49, 1935.
- (9) Ford, J. F.; Mann, C. K.; Vickers, T. J. *Appl. Spectrosc.* **1994**, 48, 592.
- (10) Chuang, E. C. C.; Lin, K. C. *J. Phys. Chem. B* **2002**, 106, 132.
- (11) Manassen, J. *J. Catal.* **1970**, 18, 38.
- (12) Noyori, R.; Umeda, I.; Kawauchi, H.; Takaya, H. *J. Am. Chem. Soc.* **1975**, 97, 812.
- (13) Taylor, R. B.; Jennings, P. W. *Inorg. Chem.* **1981**, 20, 3997.
- (14) Sen, A.; Thomas, R. R. *Organometallics* **1982**, 1, 1251.
- (15) Landis, M. E.; Gremaud, D.; Patrick, T. B. *Tetrahedron Lett.* **1982**, 23, 375.
- (16) Chalmers, J. M.; *Spectroscopy in Process Analysis*; Sheffield Academic Press: England, 2000.
- (17) Wang, C. C.; Chin, T. L.; Lin, K. C. *J. Chem. Phys.* **1997**, 107, 10348.
- (18) Chin, T. L.; Lin, K. C. *Appl. Spectrosc.* **1999**, 53, 22.
- (19) Wang, C. C.; Chen, Y. P.; Chin, T. L.; Lin, K. C. *J. Chem. Phys.* **2000**, 112, 10204.
- (20) Crank, J. *The Mathematics of Diffusion*; Oxford University Press: Ely House, London, 1975.
- (21) Karger, J.; Ruthven, D. M. *Diffusion in Zeolites and Other Microporous Solids*; Wiley Press: New York, 1992.
- (22) Lindberg, W.; Persson, J.-A. *Anal. Chem.* **1983**, 55, 643.
- (23) Phelan, M. K.; Barlow, C. H.; Kelly, J. J.; Jinguji, T. M.; Callis, J. B. *Anal. Chem.* **1989**, 61, 1419.
- (24) Schrieve, G. D.; Ullman, A. H. *Appl. Spectrosc.* **1991**, 45, 713.
- (25) Asfour, A.-F. A.; Dullien, F. A. L. *J. Chem. Eng. Data* **1981**, 26, 312.
- (26) Fan, H. F.; Chin, T. L.; Lin, K. C., to be published.